EurJIC European Journal of Inorganic Chemistry
ChemPubSoc Europe
FULL PAPER

DOI:10.1002/ejic.201200967

Platinum Complexes of 5,6-Dihydroacenaphtho[5,6-*cd*]-1,2-dichalcogenoles

Callum G. M. Benson,[a] Catherine M. Schofield,[a] Rebecca A. M. Randall,[a] Lucy Wakefield,[a] Fergus R. Knight,[a] Alexandra M. Z. Slawin,[a] and J. Derek Woollins*[a]

Keywords: Platinum complexes / Chalcogens / Metathesis / Acenaphthene

Six bis(phosphane)platinum complexes bearing dichalcogen acenaphthene ligands have been prepared by metathesis from *cis*-[$PtCl_2(PR_3)_2$] (R_3 = Ph_3, Ph_2Me, $PhMe_2$) and the dilithium salts of the parent 5,6-dihydroacenaphtho[5,6-*cd*]-1,2-dichalcogenoles ($AcenapE_2$, **L1** E = S, **L2** E = Se). For their synthesis, the appropriate disulfide or diselenide species was treated with super hydride [$LiBEt_3H$] to afford the dilithium salt by in situ reduction of the $AcenapE_2$ E–E bond. Further reaction, by metathetical addition to the *cis*-platinum precursor afforded the respective platinum(II) complexes [$Pt(5,6\text{-}AcenapE_2)(PR_3)_2$] ($R_3$ = Ph_3: E = S **1**, Se **2**; R_3 = Ph_2Me: E = S **3**, Se **4**; R_3 = $PhMe_2$: E = S **5**, Se **6**). All six complexes have been fully characterised, principally by multinuclear magnetic resonance spectroscopy, IR spectroscopy and MS. The selenium complexes **4** and **6** provide examples of AA′X spin systems, as displayed by their $^{31}P\{^1H\}$ NMR spectra. The X-ray structures of **L1**, **L2**, **1**, **2**, **5** and **6** were determined and, where appropriate, the platinum metal geometry, *peri*-atom displacement, splay angle magnitude, acenaphthene ring torsion angles and E···E interactions were analysed. The platinum atoms were found to adopt a distorted square-planar geometry in all four complexes, and the nature of the $AcenapE_2$ ligand plays little part in the conformation of the substituents bound to the trivalent phosphorus atoms.

Introduction

The coordination chemistry of *peri*-substituted naphthalenes and structurally related systems has been developed over the last 15 years.[1] Geometric constraints unique to these frameworks are imposed by a double substitution at the *peri*-positions (positions 1 and 8 of the naphthalene ring, 5 and 6 of acenaphthene),[2,3] which places large heteroatoms or groups in close proximity, usually within their van der Waals radii.[4] A number of investigators have utilised this characteristic of the naphthalene scaffold to study bonding interactions in main group systems, in which molecular geometry is determined by competition between attractive (covalent and weak) forces and repulsive interactions (steric strain).[5,6] The distinguishing feature of *peri*-substitution is the ability to achieve a relaxed geometry through the formation of a direct bond between the two *peri*-atoms.[7] Furthermore, proximity effects associated with *peri*-substitution favour complexation to bridging metal species, which provide the correct spatial arrangement for bidentate coordination.

Transition metal complexes incorporating 1,8-disubstituted naphthalene ligands have been well documented,[1] and the majority of examples reported have either bis(phosphane) or bis(thiolate) functionalities. Complexes assembled from ligands with Group 16 donor atoms invariably contain the naphthalene-1,8-dichalcogenole motif, $NapE_2$.[1] Initial investigations were undertaken by the group of Teo, who examined the extensive redox chemistry of tetrathionaphthalene (TTN), tetrachlorotetrathionaphthalene (TCTTN) and tetrathiotetracene (TTT) by preparing a series of singly and doubly bridged platinum and iridium complexes.[8] Further complexes were prepared with TTN-type ligands coordinated to Fe, Co and Ni.[9] Similarly, oxidative addition of [$Pd(PPh_3)_3$] and [$Pt(PPh_3)_4$] to the related hexachloronaphthalene-1,8-dithiole (hcdtn) ligand affords two mononuclear square-planar complexes,[10,11] and treatment with $RhCl(PPh_3)_3$ results in the formation of a five-coordinate Rh^{III} complex.[11] In comparison, the reaction of hcdtn with [$Ni(cod)_2$] and PPh_3 affords a memorable trinuclear nickel(II) complex.[10]

During our investigations of *peri*-substituted naphthalenes, we prepared a series of bis(phosphane)platinum complexes bearing dichalcogen-derivatised naphthalene, acenaphthene and phenanthrene ligands by oxidative addition to zero-valent platinum species and from metathetical methods with *cis*-[$PtCl_2(PR_3)_2$].[12] In a comparative study, we reported a series of binuclear iridium(II) complexes, which were synthesised from the oxidative reactions of similar di-

[a] EASTChem, School of Chemistry, University of St Andrews, St Andrews, Fife, KY16 9ST, UK
Fax: +44-1334-463384
E-mail: jdw3@st-and.ac.uk
Homepage: https://risweb.st-andrews.ac.uk/portal/da/persons/j-derek-woollins%28216cc072-5a91-4408-aadd-994771a4af27%29.html

Supporting information for this article is available on the WWW under http://dx.doi.org/10.1002/ejic.201200967.

thiole ligands with [{Ir(μ-Cl)(cod)}$_2$].[13] To supplement our initial platinum study, [NapS$_2$Pt(PPh$_3$)$_2$] was further treated with a range of Pt, Pd, Rh, Ir and Mo complexes to afford a series of bimetallic complexes containing an MM′S$_2$ core.[14] The corresponding reactions with [AuPPh$_3$]ClO$_4$ and AgClO$_4$ afforded binuclear and tetranuclear gold clusters and tri- or tetranuclear silver clusters; the outcome was dependent upon the stoichiometry of the reactants.[15] Further examples of multimetallic complexes bearing naphthalene dithiolate ligands have been reported in the literature, which include examples of tetra- and pentanuclear copper(I) complexes of 1,8-naphthalene dithiolate[16] and oligomeric, dimeric and monomeric zinc complexes of 2,7-di-*tert*-butylnaphtho[1,8-*c,d*][1,2]dithiole and naphthoic anhydride dithiole.[17] We have also prepared a series of titanocene complexes that incorporate a range of dithioles with modified naphthalene-1,8-yl backbones by oxidative addition reactions involving TiCp$_2$(CO)$_2$.[18] A homologous series of three Group 4 metallocene complexes was also achieved from [MCp*$_2$Cl$_2$] (M = Ti, Zr, Hf).[19]

Although the coordination chemistry of sterically crowded 1,8-disubstituted naphthalenes has been well investigated, complexes formed from related *peri*-substituted 1,2-dihydroacenaphthylenes (acenaphthene)[3] have received much less attention. Recently, we have focused on the acenaphthene skeleton and investigated chalcogen–tin compounds[20] and related halogen–chalcogen and chalcogen–chalcogen derivatives,[21] which were shown to be ideal building blocks for the construction of silver(I) coordination complexes and extended networks.[22] Herein, we describe the preparation and structural analysis of six bis(phosphane)platinum complexes [Pt(5,6-AcenapE$_2$)(PR$_3$)$_2$] (R$_3$ = Ph$_3$: E = S **1**, Se **2**; R$_3$ = Ph$_2$Me: E = S **3**, Se **4**; R$_3$ = PhMe$_2$: E = S **5**, Se **6**), which were formed by metathetical methods from 5,6-dihydroacenaphtho[5,6-*cd*]-1,2-dichalcogenoles (AcenapE$_2$, **L1** E = S, **L2** E = Se) and *cis*-[PtCl$_2$(PR$_3$)$_2$] (R$_3$ = Ph$_3$, Ph$_2$Me, PhMe$_2$; Scheme 1).

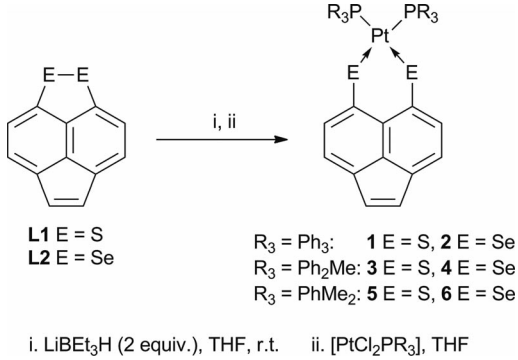

Scheme 1. Reaction scheme for the preparation of bis(phosphane) complexes [Pt(5,6-AcenapE$_2$)(PR$_3$)$_2$] **1**–**6** bearing 5,6-dihydroacenaphtho[5,6-*cd*]-1,2-dichalcogenoles **L1** and **L2**.

Results and Discussion

BisphosphanePlatinum complexes **1**–**6** bearing 5,6-dihydroacenaphtho[5,6-*cd*]-1,2-dichalcogenoles (AcenapE$_2$, **L1** E = S, **L2** E = Se) have been prepared by metathesis from *cis*-[PtCl$_2$(PR$_3$)$_2$] (R$_3$ = Ph$_3$, Ph$_2$Me, PhMe$_2$) and the dilithium salts of the parent dichalcogen acenaphthene ligands (Scheme 1). All six complexes **1**–**6** and ligands **L1** and **L2** were synthesised and fully characterised, principally by multinuclear magnetic resonance spectroscopy, IR spectroscopy and mass spectrometry. The homogeneity of the new compounds was confirmed by microanalysis where possible.

5,6-Dihydroacenaphtho[5,6-*cd*]-1,2-dithiole (AcenapS$_2$, **L1**) and 5,6-dihydroacenaphtho[5,6-*cd*]-1,2-diselenole (AcenapSe$_2$, **L2**) were prepared from 5,6-dibromoacenaphthene by following standard literature procedures.[23,24] The synthesis of the platinum metal complexes was based on previously well documented routes to complexes of 1,8-disubstituted naphthalene chalcogenides and related polyaromatic hydrocarbon compounds.[12] For their synthesis, the appropriate 5,6-dihydroacenaphtho[5,6-*cd*]-1,2-dichalcogenole was treated with two equivalents of super hydride [LiBEt$_3$H] in tetrahydrofuran at room temperature to generate a reactive dilithium intermediate by in situ reduction of the E–E bond. Subsequent metathetical addition to the desired *cis*-platinum precursor afforded the respective platinum(II) complexes [Pt(5,6-AcenapE$_2$)(PR$_3$)$_2$] (R$_3$ = Ph$_3$: E = S **1**, Se **2**; R$_3$ = Ph$_2$Me: E = S **3**, Se **4**; R$_3$ = PhMe$_2$: E = S **5**, Se **6**) in good to moderate yields (43–76%; Scheme 1).

The ^{31}P{^{1}H} NMR spectroscopic data for the series of bis(phosphane) complexes is displayed in Table 1. The spectra of complexes **1**, **3** and **5**, which bear the sulfur ligand **L1**, display the anticipated single resonances with platinum satellites, which move to lower chemical shifts as the alkyl group attached to the phosphorus atom is varied from R$_3$ = Ph$_3$ to PhMe$_2$ [**1** δ = 23.52 ppm, ^1J(^{31}P,^{195}Pt) = 2980 Hz; **3** δ = 4.51 ppm, ^1J(^{31}P,^{195}Pt) = 2926 Hz; **5** δ = –13.14 ppm ^1J(^{31}P,^{195}Pt) = 2861 Hz]. A decrease in the coupling constants of the platinum satellites is also observed from Ph$_3$ to PhMe$_2$, which is consistent with the decrease in electronegativity of the alkyl substituents and an apparent decrease in the s character of the bond.[25]

Table 1. ^{31}P{^{1}H} NMR spectroscopic data for **1**–**6**.[a]

	1	**2**	**3**	**4**	**5**	**6**
δ	23.52	20.19	4.51	1.22	–13.14	–16.22
^1J(^{31}P,^{195}Pt)	2980	3020	2926	2958	2861	2861
^2J(^{31}P,^{77}Se)	–	–	–	–	–	47(*cis*); 56(*trans*)

[a] δ in ppm, J in Hz.

The platinum complexes **2**, **4** and **6**, which contain two phosphane ligands and the symmetrical bis-selenium ligand **L2**, can be analysed as AA′X spin systems (disregarding the satellites for ^{31}P/^{77}Se–^{195}Pt coupling; Figure 1).[26] The AA′ nuclei correspond to the two ^{31}P atoms that align with either a *cis* or *trans* configuration with respect to the low abundance ^{77}Se NMR active isotope, which is the X nucleus in the spin system (Figure 1). The presence of the NMR-inactive isotopomer of the X nucleus at the second Se coordinating site breaks the symmetry of the molecule and ensures that the two ^{31}P environments are magnetically in-

equivalent. This secondary isotopomer effect, combined with the presence of weak ^{31}P–^{31}P coupling, creates a complex satellite system that is observed in both the ^{31}P and ^{77}Se NMR spectra of these compounds (Figure 1).

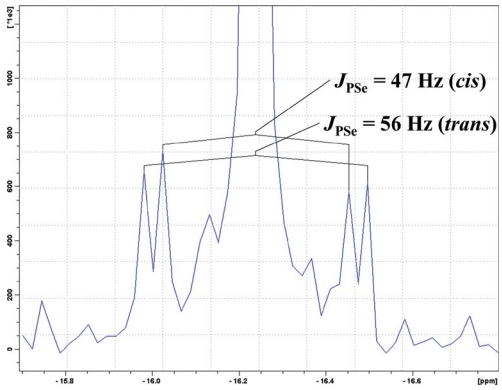

Figure 1. An expansion of the $^{31}P\{^1H\}$ NMR spectrum of **6** showing the satellites for *cis* and *trans* $^2J(^{31}P,^{77}Se)$ coupling of an AA′X spin system [the satellites for the large $^1J(^{31}P,^{195}Pt)$ coupling are omitted for clarity].

The expected AA′X pattern was not fully resolved in the $^{31}P\{^1H\}$ NMR spectrum of **4** because it was difficult to obtain data with sufficient signal-to-noise ratios. Nevertheless, the standard single resonance (corresponding to molecules containing NMR-inactive Se nuclei) was observed upfield to the signal of the equivalent sulfur complex **3** and with the expected satellites for $^1J(^{31}P,^{195}Pt)$ coupling [**4** δ = 1.22 ppm, $^1J(^{31}P,^{195}Pt)$ = 2958 Hz].

In comparison, the $^{31}P\{^1H\}$ NMR spectra of **2** and **6** display the expected pattern for the AA′ nuclei of an AA′X spin system.[26] In addition to the established single resonances accompanied by platinum satellites [**2** δ = 20.19 ppm, $^1J(^{31}P,^{195}Pt)$ = 3020 Hz; **6** δ = –16.22 ppm, $^1J(^{31}P,^{195}Pt)$ = 2861 Hz], satellites for ^{77}Se coupling are also present in both spectra. In the spectrum of **6**, two sets of ^{77}Se satellites are clearly present with $^2J(^{31}P,^{77}Se)$ values of 47 and 56 Hz, which correspond to the *cis* and *trans* couplings (Figure 1). Although it is impossible to assign the two distinct satellites as being either *trans* or *cis* to the ^{77}Se nuclei in the system, the *J* values are consistent with those found in the naphthalene analogue [Pt(1,8-Se_2-nap)-(PMe_3)$_2$] (47 and 53 Hz). In contrast, the $^2J(^{31}P,^{77}Se)$ *cis*/*trans* coupling constants for **2** are of a similar magnitude, and thus result in an overlap of the satellites in the ^{31}P NMR spectrum, which make the exact values for the two couplings difficult to extract. $^1J(^{31}P_A,^{31}P_{A'})$ coupling constants are notoriously small for AA′X spin systems[27] and were not observed in the $^{31}P\{^1H\}$ NMR spectra of **2**, **4** and **6**. The partial solubility of the complexes also made it problematic to obtain ^{77}Se NMR spectra with reasonable signal-to-noise ratios for these complexes.

X-ray Investigations

Crystals of **L1** and **L2** suitable for X-ray diffraction were obtained by cooling a hot hexane solution to –10 °C overnight. In addition, single crystals of **1**, **2**, **5** and **6** were obtained by diffusion of hexane into saturated solutions of the individual compounds in dichloromethane. The selenium ligand **L2** contains two nearly identical molecules in the asymmetric unit; all other compounds contain one molecule in the asymmetric unit. Selected interatomic distances, angles and torsion angles are listed in Tables 2 and 3. Further crystallographic information can be found in Table 4 and in the Supporting Information.

5,6-Dihydroacenaphtho[5,6-*cd*]-1,2-dichalcogenoles [AcenapE_2, **L1** (E = S) and **L2** (E = Se), Figure 2) unsurprisingly adopt similar molecular structures to those of their naphthalene equivalents NapE_2.[29] Nevertheless, the introduction of the ethane linkage at the 1,2-positions in the acenaphthene molecule naturally reduces the C4–C5–C6 bond angle (**L1**/**L2** 114/113°; cf. NapS_2/NapSe_2 125/123°)[29] and simultaneously increases the C1–C10–C9

Table 2. Selected interatomic distances [Å] and angles [°] for **L1**, **L2**, **1**, **2**, **5**, **6**.

Ligand; *peri* atoms	**L1** SS	**L2** SeSe	**1** **L1**; SS	**2** **L2**; SeSe	**5** **L1**; SS	**6** **L2**; SeSe
E(1)···E(9)	2.1025(19)	2.400(2) [2.380(2)]	3.267(4)	3.437(3)	3.273(7)	3.418(3)
Σr_{vdW}–E(1)···E(9);[a] $\%\Sigma r_{vdW}$	1.498; 58	1.400; 63 [1.420; 63]	0.333; 91	0.363; 90	0.325; 91	0.381; 90
peri-Region bond angles						
E(1)–C(1)–C(10)	113.6(3)	114.0(9) [117.4(9)]	125.7(7)	127.2(12)	127.1(11)	131.0(10)
C(1)–C(10)–C(9)	120.2(5)	128.0(11) [122.6(11)]	128.9(8)	128.0(13)	128.7(12)	129.5(11)
E(9)–C(9)–C(10)	114.4(4)	114.9(9) [116.3(10)]	127.9(6)	130.5(10)	128.0(11)	125.9(10)
Sum of bay angles	348.2(7)	356.9(17) [356.3(17)]	382.5(12)	385.7(20)	383.8(20)	386.4(18)
Splay angle[b]	–11.8	–3.1 [-3.7]	22.5	25.7	23.8	26.4
Out-of-plane displacement						
E(1)	0.022(1)	–0.053(1) [-0.061(1)]	0.170(1)	0.155(1)	0.044(1)	0.157(1)
E(9)	0.003(1)	–0.032(1) [0.023(1)]	0.075(1)	0.015(1)	0.127(1)	0.014(1)
Central naphthalene ring torsion angles						
C:(6)–(5)–(10)–(1)	179.84(1)	178.96(1) [177.76(1)]	177.98(1)	178.51(1)	179.37(1)	177.36(1)
C:(4)–(5)–(10)–(9)	179.55(1)	178.69(1) [177.07(1)]	–179.97(1)	178.25(1)	178.04(1)	173.18(1)

[a] Van der Waals radii used for calculations: r_{vdW}(S) 1.80 Å, r_{vdW}(Se) 1.90 Å.[28] [b] Splay angle: Σ of the three bay region angles – 360.

Table 3. Platinum coordination geometry; selected intramolecular distances [Å] and angles [°] for **1**, **2**, **5**, **6**.

Complex	**1**	**2**	**5**	**6**
Ligand; *peri* atoms	**L1**; SS	**L2**, SeSe	**L1**; SS	**L2**, SeSe
Metal geometry – bond lengths				
E(1)–Pt(1)	2.336(2)	2.4558(16)	2.324(4)	2.449(3)
E(9)–Pt(1)	2.323(3)	2.4356(16)	2.324(5)	2.438(3)
P(1)–Pt(1)	2.301(2)	2.304(4)	2.258(5)	2.279(4)
P(2)–Pt(1)	2.295(2)	2.294(4)	2.267(4)	2.277(5)
Metal geometry – bond angles				
E(1)–Pt(1)–E(9)	89.07(8)	89.27(6)	89.61(15)	88.78(6)
E(1)–Pt(1)–P(1)	86.53(8)	86.47(10)	84.53(15)	86.60(11)
P(1)–Pt(1)–P(2)	97.51(8)	97.68(13)	100.84(15)	100.45(14)
E(9)–Pt(1)–P(2)	87.54(8)	87.56(10)	85.47(14)	84.67(11)
E(1)–Pt(1)–P(2)	172.20(9)	170.63(12)	173.00(16)	171.08(10)
E(9)–Pt(1)–P(1)	172.79(8)	171.95(11)	171.87(13)	173.09(12)
Metal geometry – distortion				
E_2Pt–P(1) distance	0.229(1)	0.274(1)	0.220(1)	–0.204(1)
E_2Pt–P(2) distance	–0.281(1)	–0.351(1)	–0.196(1)	0.240(1)
Envelope geometry				
E_2C_3–Pt angle	135.92(1)	139.16(1)	134.44(1)	133.77(1)
E_2C_3–Pt distance	1.152(1)	1.137(1)	1.175(1)	1.259(1)

angular splay (**L1**/**L2** 120/128°; cf. $NapS_2$/$NapSe_2$ 118/122°),[29] which consequently elongates the short S–S and Se–Se *peri* bonds in these "simple" single-bonded systems {**L1** 2.1025(19) Å, cf. $NapS_2$ 2.0879(8) Å; **L2** 2.400(2) Å [2.380(2) Å], cf. $NapSe_2$ 2.3639(5) Å}.[29] The steric demands imposed by the substitution of heavy chalcogen atoms are relieved in these systems by the formation of such strong E–E covalent bonds, regardless of the minor increase in their length. In the sulfur analogue **L1**, this is accompanied by a large negative splay angle as the exocyclic *peri* bonds naturally converge (–11.8°, cf. $NapS_2$ –11.2°), and there is only a minor displacement of the sulfur atoms from the mean plane of the organic backbone, in line with the naphthalene compound (0.01–0.02 Å).[29] Typical for systems incorporating larger substituents, the selenium counterpart **L2** exhibits a more positive splay angle (–3.1° [–3.7°], cf. $NapSe_2$ –3.6°),[29] and the two E–C_{Acenap} bonds now adopt a more parallel alignment. Buckling of the two naturally planar carbon frameworks is minimal and comparable to that observed in the naphthalene compounds; the greatest distortion is observed in the selenium analogue **L2**, which has maximum C–C–C–C central acenaphthene torsion angles in the range 178–179°.

Treatment of the dilithium salts of **L1** and **L2** with *cis*-[$PtCl_2(PPh_3)_2$] afforded two isomorphous monomeric, mononuclear four coordinate platinum(II) complexes [Pt(5,6-AcenapE_2)(Ph_3)$_2$] (**1** E = S; **2** E = Se; Figure 3). Similarly, the corresponding reactions with *cis*-[$PtCl_2(PPhMe_2)_2$] generated a pair of equivalent isomorphous platinum(II) complexes [Pt(5,6-AcenapE_2)($PhMe_2$)$_2$] (**5** E = S; **6** E = Se; Figure 4). In each case, the symmetrical bidentate dichalcogen ligand binds through both E atoms to form a chelate ring with the central metal atom. The PtE_2C_3 six-membered rings are hinged about the E···E vector and adopt a twisted envelope-type conformation (Figure 5); E(1), E(9), C(1), C(10) and C(9) are essentially coplanar, the platinum atom in the *peri* gap is displaced 1.15–1.26 Å above the E_2C_3 plane, and the E(1)–Pt(1)–E(9) plane is inclined by 134–139°.

As a consequence of the ligand geometry, the two phosphane moieties retain a *cis* orientation around the platinum atom and complete a distorted square-planar geometry. The P(1)–Pt(1)–P(2) angles for **1** [97.51(8)°] and **2** [97.68(13)°], which bear the PPh_3 moiety, show considerable deviation from the ideal 90° in accord with previously published examples. Counterintuitively, even larger angles are exhibited by **5** [100.84(15)°] and **6** [100.45(14)°], despite the incorporation of the less sterically hindered $PPhMe_2$ functionality, which is associated with a smaller Tolman cone angle ($PPhMe_2$ 136° cf. PPh_3 145°).[30] In contrast, the corresponding E(1)–Pt(1)–E(9) angles in all four complexes are consistent with angles in the range 88.78(6)–89.61(15)°. The *cis* E(1)–Pt(1)–P(1), E(9)–Pt(1)–P(2) [84.53(15)–87.56(10)°] and *trans* E(1)–Pt(1)–P(2), E(9)–Pt(1)–P(1) angles [170.63(12)–173.09(12)°] also fall within accepted ranges for similar platinum complexes[12,27] but highlight the distortion of the square planar environment at the central platinum core. The Pt–S [2.323(3)–2.336(2) Å], Pt–Se [2.436(2)–2.456(2) Å] and Pt–P [2.258(5)–2.304(4) Å] bond lengths correspond to distances seen in previous naphthalene complexes.[12,27] In addition to the in-plane deviations, further distortion is observed in all four complexes; out-of-plane displacement of the coordinating E and P atoms reduces the planarity of the primary coordination sphere of the platinum atom. This can be compared by monitoring the location of the P atoms with respect to the mean E–Pt–E plane (Figure 6). In each case E(1), Pt(1) and E(9) are essentially coplanar, and the P atoms are displaced to opposite sides of this plane by 0.2–0.4 Å (Figure 6). The C–E–Pt bond angles are found to decrease from PPh_3 to

Table 4. Crystallographic data for **L1**, **L2**, **1**, **2**, **5**, **6**.

	L1	**L2**	**1**
Empirical formula	$C_{12}H_8S_2$	$C_{12}H_8Se_2$	$C_{48}H_{38}P_2PtS_2$
Formula weight	216.32	310.12	935.99
Temperature [°C]	–148(1)	–148(1)	–180(1)
Crystal colour, habit	orange, platelet	green, platelet	orange, prism
Crystal dimensions [mm^3]	0.09 × 0.09 × 0.03	0.30 × 0.30 × 0.02	0.20 × 0.20 × 0.20
Crystal system	monoclinic	monoclinic	monoclinic
Lattice parameters	a = 13.871(8) Å	a = 7.359(5) Å	a = 9.769(3) Å
	b = 4.952(3) Å	b = 21.383(14) Å	b = 17.571(5) Å
	c = 14.633(7) Å	c = 12.304(9) Å	c = 22.605(6) Å
	β = 116.097(12)°	β = 99.016(19)°	β = 102.379(7)°
Volume [Å^3]	902.7(8)	1912(2)	3790(2)
Space group	$P2_1/n$	$P2_1/n$	$P2_1/n$
Z	4	8	4
$D_{calcd.}$ [g cm^{-3}]	1.592	2.154	1.640
F(000)	448	1184	1864
λ(Mo-K_α) [cm^{-1}]	5.346	76.842	39.177
Number of reflections measured	7383	15458	23502
R_{int}	0.0660	0.1143	0.1206
Min/max. transmissions	0.765/0.984	0.442/0.858	0.201/0.457
Observed reflection (number of variables)	2055(127)	3850(253)	6898(466)
Reflection/parameter ratio	16.18	15.22	14.80
Residuals: R_1 [$I > 2\sigma(I)$]	0.0904	0.0981	0.0701
Residuals: R (all reflections)	0.1297	0.1337	0.0884
Residuals: wR_2 (all reflections)	0.2913	0.2569	0.1938
Goodness-of-fit indicator	1.133	1.240	1.069
Maximum peak in final diff. map [e Å^{-3}]	1.63	1.40	2.06
Minimum peak in final diff. map [e Å^{-3}]	–1.01	–1.85	–3.40
	2	**5**	**6**
Empirical formula	$C_{48}H_{38}P_2PtSe_2$	$C_{28}H_{30}P_2PtS_2$	$C_{28}H_{30}P_2PtSe_2$
Formula Weight	1029.79	687.70	781.50
Temperature [°C]	–180(1)	–148(1)	–148(1)
Crystal colour, habit	orange, prism	orange, platelet	orange, plate
Crystal dimensions [mm^3]	0.10 × 0.10 × 0.03	0.17 × 0.08 × 0.02	0.15 × 0.15 × 0.09
Crystal system	monoclinic	triclinic	triclinic
Lattice parameters	a = 9.797(4) Å	a = 9.978(3) Å	a = 10.111(7) Å
	b = 17.656(5) Å	b = 11.416(4) Å	b = 11.637(11) Å
	c = 22.821(8) Å	c = 11.731(4) Å	c = 11.678(10) Å
	–	α = 106.918(9)°	α = 106.30(3)°
	β = 101.690(8)°	β = 92.914(10)°	β = 94.62(2)°
	–	γ = 95.035(9)°	γ = 93.48(3)°
Volume [Å^3]	3865(3)	1269.4(7)	1310(2)
Space group	$P2_1/n$	$P\bar{1}$	$P\bar{1}$
Z	4	2	2
$D_{calcd.}$ [g cm^{-3}]	1.769	1.799	1.982
F(000)	2008	676	748
λ(Mo-K_α) [cm^{-1}]	56.169	58.114	82.538
No. of reflections measured	24021	8862	11373
R_{int}	0.1944	0.0909	0.0604
Min./max. transmissions	0.306/0.845	–	0.271/0.476
Observed reflection (number of variables)	7007(459)	4268(298)	5707(298)
Reflection/parameter ratio	15.27	14.32	19.15
Residuals: R_1 [$I > 2\sigma(I)$]	0.0898	0.0771	0.0611
Residuals: R (all reflections)	0.1314	0.0918	0.0911
Residuals: wR_2 (all reflections)	0.2369	0.1529	0.2645
Goodness-of-fit indicator	1.052	1.193	1.039
Maximum peak in final diff. map [e Å^{-3}]	1.83	1.57	2.28
Minimum peak in final diff. map [e Å^{-3}]	–2.24	–2.97	–4.62

$PPhMe_2$; the average angles for **1** and **2** are 111° and 109° for **5** and **6**. The reduction in the C–E–Pt angle is consistent with the smaller functionality on the phosphorus atom, which allows the platinum atom to lie closer to the acenaphthene framework.

The arrangement of substituents in trivalent phosphorus ligands is dictated by steric effects; R–P–R′ angles are commonly less than 109.5° and approach an ideal tetrahedral geometry as bulky groups are added.[30] In **1**, **2**, **5** and **6**, the nature of the $AcenapE_2$ ligand has no apparent effect

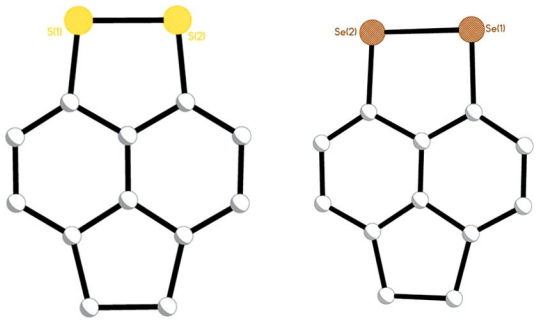

Figure 2. The molecular structures of 5,6-dihydroacenaphtho[5,6-*cd*]-1,2-dichalcogenoles (AcenapE$_2$, **L1** E = S, **L2** E = Se; H atoms omitted for clarity).

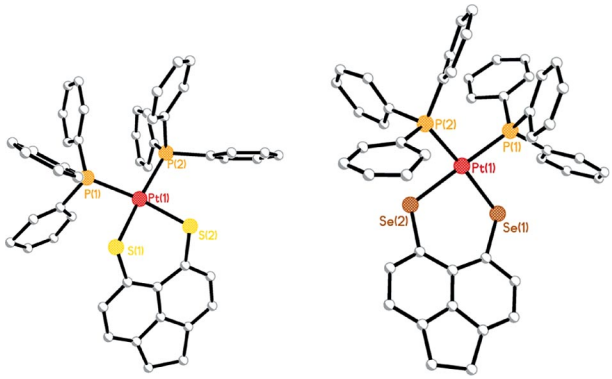

Figure 3. The molecular structures of **1** and **2** formed from *cis*-[PtCl$_2$(PPh$_3$)$_2$] and bearing chalcogen ligands **L1** and **L2** (H atoms omitted for clarity).

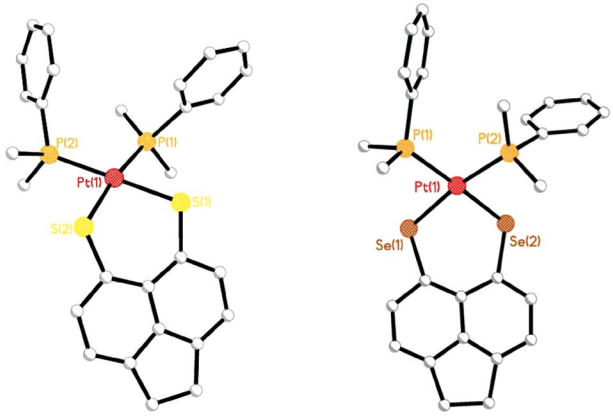

Figure 4. The molecular structures of **5** and **6** formed from *cis*-[PtCl$_2$(PPhMe$_2$)$_2$] (H atoms omitted for clarity).

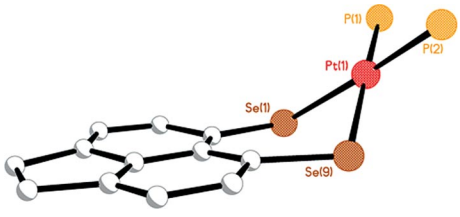

Figure 5. The open-envelope configuration of the six-membered chelate ring formed from bidentate Se coordination of **L2** in **6** (phenyl and methyl groups and H atoms omitted for clarity).

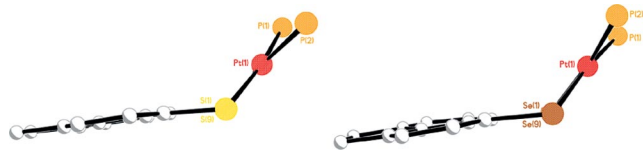

Figure 6. Out-of-plane distortion of the square-planar geometry in **5** and **6**; displacement of the P atoms from the mean E–Pt–E plane (phenyl and methyl groups and H atoms omitted for clarity).

on the conformation of the phosphorus moiety, and the R–P–R angles are comparable for **1** (av. 103.5°) and **2** (av. 103.7°), and **5** (av. 102.3°) and **6** (av. 102.8). Although the average of the C_{Ph}–P–C_{Ph} angles in **1** and **2** (104°) is closer to that of a standard tetrahedral arrangement (as expected for larger substituents),[30] the angles range between 97.6(4) and an unusually large 111.8(4)° [cf. **5/6** 99.6(6)–105.8(8)°]. As might be expected from the larger steric influence of the PPh$_3$ group compared with that of PPhMe$_2$, longer Pt–P bonds are observed in **1** and **2** (av. 2.30 Å) than in **5** and **6** (2.27 Å). Although steric effects dominate the configuration of the substituents around the phosphorus atoms, weak interactions between the functional groups of neighbouring phosphorus atoms can influence the structure of the complex. In **1** and **2**, two neighbouring phenyl rings attached to independent P atoms adopt a parallel alignment similar to the face-to-face offset arrangement (Figure 7)[31] and have nonbonded distances between the interacting centroids [cg(C25–C30)···cg(C31–C36): **1** 3.765(1) Å; **2** 3.764(1) Å] within the range for typical π···π stacking (3.3–3.8 Å).[31] Similarly, **5** and **6** exhibit weak nonconventional CH···π-type hydrogen bond interactions[32] between neighbouring methyl and phenyl moieties of adjacent phosphorus groups [**5** C(14)–H(14C)···cg(C23–C28) 2.61 Å; **6** C(21)–H(21A)···cg(C15–C20) 2.72 Å; Figure 8].

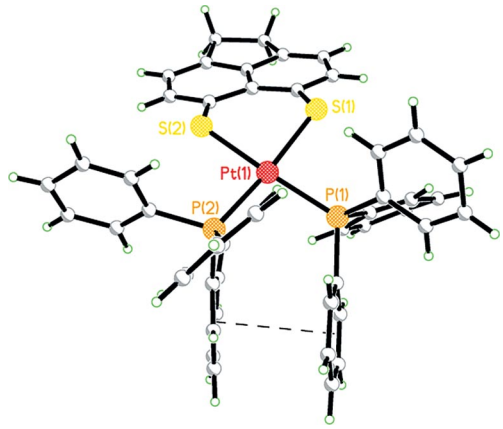

Figure 7. Overlapping phenyl rings in the isomorphous complexes **1** (shown) and **2** align with a weak face-to-face offset arrangement and interact through weak π···π stacking.

Unsurprisingly, cleavage of the short E–E covalent bond and subsequent coordination to the platinum centre in **1**, **2**, **5** and **6** causes steric strain to accumulate between the bulky chalcogen atoms. The repulsive interactions between the two *peri* functionalities that result from sub-van-der-Waals

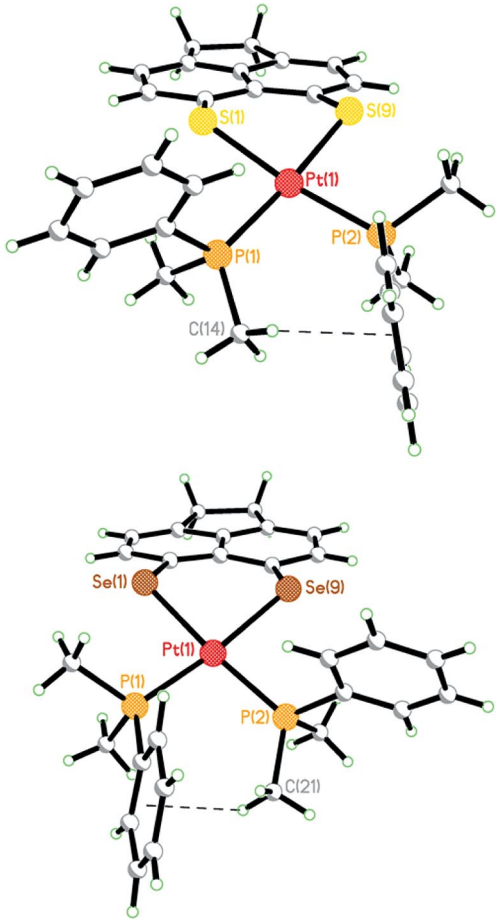

Figure 8. Adjacent phenyl and methyl moieties interact in **5** (top) and **6** (bottom) through weak nonconventional CH···π-type interactions.

contacts lead to deformation of the carbon framework by in-plane and out-of-plane distortions and buckling of the aromatic ring system (angular strain), which ultimately disrupts the relaxed geometry previously achieved by the free ligands. As a consequence of the square planar metal geometry, the exocyclic E–C_{Acenap} bonds now diverge, which results in large positive splay angles in the range 23–26° and extended nonbonded E···E distances more than 1 Å longer than the E–E distances in the $AcenapE_2$ ligands [**1** 3.267(4), **5** 3.273(7); cf. **L1** 2.1025(19); **2** 3.437(3), **6** 3.418(3); cf. **L2** 2.400(2) Å]. This is accompanied by an increase in the out-of-plane displacement of the *peri* atoms (0–0.2; cf. **L1/L2** 0–0.05 Å) and a reduction in the planarity of the carbon skeleton (C–C–C–C torsion angles 0.1–7°; cf. **L1/L2** 0–0.1°). As can be seen from the magnitude of the E···E *peri* separations, the subtle change of the phosphorus functionality from PPh_3 to $PPhMe_2$ has only a minor effect on the geometry of the acenaphthene fragment in these complexes. The most notable difference is observed within the bay region, and marginally larger splay angles are exhibited by **2** and **6** ($PPhMe_2$), which are ca. 1° larger than those of **1** and **5** (PPh_3). Naturally, the selenium analogues **2** and **6** exhibit greater molecular distortion within the acenaphthene fragment and longer *peri* E···E distances compared with those of sulfur equivalents **1** and **5**, in line with the greater bulk of the interacting atoms.

During an earlier study of bis(phosphane)platinum complexes bearing a range of dichalcogen derivatised naphthalene, acenaphthene and phenanthrene ligands, we prepared [Pt(1,8-$NapSe_2$)(PPh_3)$_2$] **N2**, which is the naphthalene analogue of **2**.[12] Although both compounds adopt comparable structures in the solid state, the introduction of the ethane linkage at the 1,2-positions of **2** has a noticeable influence on the geometry of the phosphorus atom and the degree of molecular distortion in the organic backbone compared with those of **N2**. The greatest discrepancy between the two compounds is found in the planarity of the organic frameworks; significantly less buckling is observed within the acenaphthene ring system of **2** (maximum C–C–C–C central ring torsion angles ca. 2°; cf. **N2** ca. 1–5°).[12] A reduction in out-of-plane distortion is associated with this is; one of the selenium atoms in **2** essentially resides on the mean acenaphthene plane, and the second atom is displaced by only ca. 0.1 Å (cf. **N2** both Se atoms displaced ca. 0.2 Å from the mean naphthalene plane).[12] The natural splay of the exocyclic bonds in acenaphthene compounds compared with those of their naphthalene equivalents accounts for the larger in-plane distortion observed in **2** (splay angle: 25.7°; cf. **N2** 23.8° [20.0°]), which results in a minor lengthening of the Se···Se separation {**2** 3.437(3) Å; **N2** 3.37(1) Å [3.36(1) Å]}.[12]

Although the in-plane Se–Pt–Se (86–89°), Se–Pt–P (86–89°) and P–Pt–P (98–99°) angles are comparable in both complexes, the out-of-plane displacement (metal geometry) of the two P atoms with respect to the Se_2Pt plane is marginally greater in the naphthalene analogue (ca. 0.4–0.5 Å; cf. **2** 0.2–0.3 Å).[12] As might be expected, the PPh_3 groups in **2** adopt a similar configuration to those found in the naphthalene analogue, and both complexes have comparable R–P–R angles (98–113°). Interestingly, although the neighbouring phenyl rings of complex **N2** overlap, the distance between the two interacting centroids {4.167(1) Å [4.166(1) Å]} is outside the range for standard π···π stacking (3.3–3.8 Å).[12,31]

Conclusions

The work presented in this paper builds on our previous studies of bis(phosphane)platinum complexes bearing dichalcogenide based ligands.[12] Herein, we present the synthesis of a related series of platinum complexes **1**–**6** that incorporate 5,6-dihydroacenaphtho[5,6-*cd*]-1,2-dichalcogenoles [$AcenapE_2$, **L1** (E = S), **L2** (E = Se)] and *cis*-[$PtCl_2(PR_3)_2$] (R_3 = Ph_3, Ph_2Me, $PhMe_2$). For their synthesis, the appropriate disulfide or diselenide species was treated with super hydride [$LiBEt_3H$] to afford the dilithium salt by in situ reduction of the $AcenapE_2$ E–E bond. Further reaction by metathetical addition to the *cis*-platinum precursor afforded the respective platinum(II) complex [Pt(5,6-$AcenapE_2$)(PR_3)$_2$] (R_3 = Ph_3: E = S **1**, Se **2**; R_3 = Ph_2Me: E = S **3**, Se **4**; R_3 = $PhMe_2$: E = S **5**, Se **6**). The

sulfur complexes **1**, **3** and **5** display the expected single resonances with platinum satellites in their $^{31}P\{^{1}H\}$ NMR spectra, which move to lower chemical shifts with decreasing $^{1}J(^{31}P,^{195}Pt)$ coupling constants as the alkyl group on the phosphorus atom is varied from $R_3 = Ph_3$ to $PhMe_2$. The inclusion of the low abundance ^{77}Se NMR active isotope in complexes **2**, **4** and **6** provides extra complexity to their $^{31}P\{^{1}H\}$ NMR spectra. These can be analysed as AA′X systems if the satellites for $^{31}P/^{77}Se$–^{195}Pt coupling are disregarded.[26] The AA′ nuclei correspond to the two ^{31}P atoms that align with either a *cis* or *trans* configuration with respect to the X nucleus in the spin system (the ^{77}Se NMR active isotope), which makes them magnetically inequivalent. The $^{31}P\{^{1}H\}$ NMR spectra of **6** displays the expected pattern for the AA′ nuclei of an AA′X spin system;[26] in addition to the established single resonance accompanied by satellites for $^{1}J(^{31}P,^{195}Pt)$ coupling, two sets of ^{77}Se satellites are clearly present and have $^{2}J(^{31}P,^{77}Se)$ values of 47 and 56 Hz for the *cis* and *trans* couplings. $^{1}J(^{31}P_A,^{31}P_{A'})$ coupling constants are notoriously small for AA′X spin systems and were not observed in the spectra of **2**, **4** and **6**.[27]

The X-ray structures were determined for **1**, **2**, **5** and **6**, and the platinum metal geometry, *peri*-atom displacement, splay angle magnitude, acenaphthene ring torsion angles and E···E interactions were analysed and compared to those of the free ligands **L1** and **L2**. In each complex, the symmetrical bidentate $AcenapE_2$ ligand coordinates to the platinum atom to form a six-membered chelate ring that adopts a twisted envelope-type motif. The two phosphane ligands retain a *cis* orientation around the platinum atom, which is at the centre of a distorted square-planar environment. Naturally, the coordination to platinum and cleavage of the E–E bond results in a dramatic increase in molecular distortion in the acenaphthene component of **1**, **2**, **5** and **6** compared with those of the free ligands **L1** and **L2**. Divergence of the exocyclic bonds results in large positive splay angles in the range 23–26° and extended nonbonded E···E distances that are 1 Å longer than the E–E distances in the $AcenapE_2$ ligands. The nature of the $AcenapE_2$ ligand has no apparent effect on the conformation of the phosphorus moiety, and **1** and **2**, and **5** and **6** have comparable R–P–R angles. Similarly, the subtle change of the phosphorus functionality from PPh_3 to $PPhMe_2$ has only a minor effect on the geometry of the acenaphthene fragment in these complexes.

Experimental Section

General: All experiments were carried out under an oxygen- and moisture-free nitrogen atmosphere using standard Schlenk techniques and glassware. Reagents were obtained from commercial sources and used as received. Dry solvents were collected from an MBraun solvent system. Elemental analyses were performed by Stephen Boyer at the London Metropolitan University. Infrared spectra were recorded as KBr discs in the range 4000–300 cm^{-1} with a Perkin–Elmer System 2000 Fourier transform spectrometer. ^{1}H and ^{13}C NMR spectra were recorded with a Jeol GSX 270 MHz spectrometer with δ(H) and δ(C) referenced to external tetramethylsilane. ^{31}P and ^{77}Se NMR spectra were recorded with a Jeol GSX 270 MHz spectrometer with δ(P) and δ(Se) referenced to external phosphoric acid and dimethylselenide, respectively. Assignments of ^{13}C and ^{1}H NMR spectra were made with the help of H–H COSY and heteronuclear single quantum coherence (HSQC) experiments. All measurements were performed at 25 °C. All values reported for NMR spectroscopy are in parts per million (ppm). Coupling constants (*J*) are given in Hertz [Hz]. Mass spectrometry was performed by the University of St. Andrews Mass Spectrometry Service; Electrospray mass spectrometry (ESMS) was carried out with a Micromass LCT orthogonal accelerator time of flight mass spectrometer. Platinum metal precursors *cis*-$[PtCl_2(PR^3)]$ ($R^3 = Ph_3$, Ph_2Me, $PhMe_2$) were prepared following standard literature procedures.[12]

5,6-Dihydroacenaphtho[5,6-*cd*][1,2]dithiole [$AcenapS_2$] (L1): The title compound was prepared by a method previously described.[23] To a stirred solution of 5,6-dibromoacenaphthene (5.0 g, 16.03 mmol) and tetramethylethylenediamine (TMEDA, 4.8 mL, 16.03 mmol) in diethyl ether (200 mL) was slowly added a hexane solution of *n*-butyllithium (2.5 M, 6.4 mL, 16.03 mmol) at –78 °C. After the mixture was stirred for 15 min at this temperature, sulfur flowers (0.51 g, 16.03 mmol) were added and stirring was continued at –40 °C for 2 h. The mixture was cooled again to –78 °C, after which a hexane solution of *n*-butyllithium (2.5 M, 6.4 mL, 16.03 mmol) was added and the reaction mixture was stirred at this temperature for 15 min. Additional sulfur (0.51 g, 16.03 mmol) was added and the reaction mixture was stirred for a further 2 h at –40 °C. The mixture was then quenched with acetic acid (2 mL) and exposed to an air stream overnight for oxidation. The resulting solution was concentrated under reduced pressure and after water was added, the mixture was extracted with dichloromethane. The extract was dried with anhydrous magnesium sulfate. After the solvent was removed in vacuo, the residue was purified by column chromatography on silica gel (hexane). An analytically pure sample was obtained by recrystallisation from hexane to give the desired product as orange crystals (0.70 g, 20%); m.p. 178–182 °C. $C_{12}H_8S_2$ (216.32): calcd. C 66.6, H 3.7; found C 66.5, H 3.8. ^{1}H NMR (270 MHz, $CDCl_3$, 25 °C, Me_4Si): δ = 7.06 (d, $^{3}J_{HH}$ = 7.5 Hz, 1 H, acenaph. 4,7-H), 7.02 (d, $^{3}J_{HH}$ = 7.2 Hz, 1 H, acenaph. 3,8-H), 3.29 (s, 4 H, 2× CH_2) ppm. ^{13}C NMR (67.9 MHz, $CDCl_3$, 25 °C, Me_4Si): δ = 121.1 (s), 116.9 (s), 30.7 (s,CH_2) ppm. (ES^+): *m/z* 215.87 ($[M]^+$, 100%).

5,6-Dihydroacenaphtho[5,6-*cd*][1,2]diselenole [$AcenapSe_2$] (L2): The title compound was prepared by a method previously described.[23] To a stirred solution of 5,6-dibromoacenaphthene (2.62 g, 8.40 mmol) and TMEDA (2.5 mL, 16.1 mmol) in diethyl ether (200 mL) was slowly added a 2.5 M hexane solution of *n*-butyllithium (3.4 mL, 8.40 mmol) at –78 °C. After the mixture was stirred for 15 min at this temperature, selenium powder (0.66 g, 8.40 mmol) was added and stirring was continued at –40 °C for 2 h. The mixture was cooled again to –78 °C, after which a 2.5 M hexane solution of *n*-butyllithium (3.4 mL, 8.40 mmol) was added and the reaction mixture stirred at this temperature for 15 min. Additional selenium powder (0.66 g, 8.40 mmol) was added and the reaction mixture stirred for a further 2 h at –40 °C. The mixture was then quenched with acetic acid (2 mL) and exposed to an air stream overnight for oxidation. The resulting solution was concentrated under reduced pressure and after water was added, the mixture was extracted with dichloromethane. The extract was dried with anhydrous magnesium sulfate. After the solvent was removed in vacuo, the residue was purified by column chromatography on silica gel (hexane/dichloromethane). An analytically pure sample was

obtained by recrystallization from boiling toluene to give the desired product as green crystals (0.83 g, 32%); m.p. 198–200 °C. $C_{12}H_8Se_2$ (310.12): calcd. C 46.5, H 2.6; found C 46.5, H 2.6. ^{1}H NMR (270 MHz, $CDCl_3$, 25 °C, Me_4Si): δ = 7.21 (d, $^3J_{H,H}$ = 7.4 Hz, 1 H, acenaph. 4,7-H), 7.05 (d, $^3J_{H,H}$ = 7.2 Hz, 1 H, acenaph. 3,8-H), 3.26 (s, 4 H, 2× CH_2) ppm. ^{13}C NMR (67.9 MHz, $CDCl_3$, 25 °C, Me_4Si): δ = 121.7 (s), 121.2(s), 30.4 (s, acenaph. CH_2) ppm. ^{77}Se NMR (51.5 MHz, $CDCl_3$, 25 °C, Me_2Se): δ = 424 (s) ppm. MS(ESI+): *m*/*z* (%) = 311.90 (100) $[M + H]^+$, 309.91 (70) $[M]^+$.

[Pt(PPh$_3$)$_2$L1] (1): Super hydride (1.1 mL of a 1.0 M solution in THF, 1.1 mmol) was added in one portion to a solution of 5,6-dihydroacenaptho[5,6-*cd*][1,2]dithiole (acenaph.S_2) **L1** (0.12 g, 0.56 mmol) in THF (20 mL). A colour change from bright red to pale yellow was observed, along with a small evolution of gas. The solution was transferred with a syringe to a suspension of *cis*-[$PtCl_2(PPh_3)_2$] (0.45 g, 0.56 mmol) in THF (10 mL) and stirred for 2 d to give a yellow solution. The mixture was filtered through a silica pad and eluted with dichloromethane (100 mL). The filtrate was evaporated to dryness under reduced pressure and redissolved in a minimum amount of dichloromethane (ca. 10 mL). Diethyl ether (25 mL) and hexane (50 mL) were added slowly to induce precipitation. The resulting microcrystalline solid was collected by filtration and was washed with diethyl ether to yield the product as a light orange powder (0.4 g, 74%); m.p. 282–284 °C. $C_{48}H_{38}P_2PtS_2$ (935.99): calcd. C 61.6, H 4.1; found C 61.4, H 4.0. ^{1}H NMR (400 MHz, $CDCl_3$, 25 °C, Me_4Si): δ = 7.48–7.38 (m, 12 H, P*Ph* 12,16-H), 7.34–7.26 (m, 6 H, P*Ph* 14-H), 7.27 (d, $^3J_{H,H}$ = 7.3 Hz, 2 H, acenaph. 4,7-H), 7.14 (td, $^3J_{H,H}$ = 7.7, $^4J_{H,H}$ = 1.8 Hz, 12 H, P*Ph* 13,18-H), 6.90 (d, $^3J_{H,H}$ = 7.3 Hz, 2 H, acenaph. 3,8-H), 3.17 (s, 4 H, acenaph.-CH_2) ppm. ^{13}C NMR (75 MHz, $CDCl_3$, 25 °C, Me_4Si): δ = 142.0 (s), 140.7 (s), 135.4–134.8 (m), 130.4 (s), 128.6–127.4 (m), 119.7 (s), 30.9 (s,CH_2) ppm. ^{31}P NMR (109 MHz, $CDCl_3$, 25 °C, H_3PO_4): δ = 23.5 ($J_{P,Pt}$ = 2980 Hz) ppm. MS(ESI+): *m*/*z* (%) = 826.66 (100) $[M – SPh]^+$.

[Pt(PPh$_3$)$_2$L2] (2): Complex **2** was prepared following a similar procedure described for **1** but with super hydride (1.1 mL, 1.1 mmol), **L2** (0.18 g, 0.56 mmol) and *cis*-[$PtCl_2(PPh_3)_2$] (0.45 g, 0.56 mmol). The resulting solid was removed by filtration, washed with toluene (5 mL) and diethyl ether (2 × 10 mL) and dried in vacuo to yield an orange powder (0.3 g, 54%); m.p. 185–186 °C. $C_{48}H_{38}P_2PtSe_2$ (1029.79): calcd. C 56.0, H 3.7; found C 55.9, H 3.8. ^{1}H NMR (400 MHz, $CDCl_3$, 25 °C, Me_4Si): δ = 7.51 (d, $^3J_{H,H}$ = 7.28 Hz, 2 H, acenaph. 4,7-H), 7.48–7.39 (m, 12 H, P*Ph* 12,16-H), 7.35–7.26 (m, 6 H, P*Ph* 14-H), 7.10 (t, $^3J_{H,H}$ = 7.06 Hz, 12 H, P*Ph* 13,18-H), 6.81 (d, $^3J_{H,H}$ = 7.25 Hz, 2 H, acenaph. 3,8-H), 3.13 (s, 4 H, 2× CH_2) ppm. ^{13}C NMR (67.9 MHz. $CDCl_3$; 25 °C; Me_4Si): δ = 143.2 (s), 143.7 (t, *J* = 5.4 Hz), 130.0 (s), 128.0 (t, *J* = 5.2 Hz), 119.3 (s), 30.1 (s, CH_2) ppm. ^{31}P NMR (109 MHz, $CDCl_3$, 25 °C, H_3PO_4): δ = 20.2 ($J_{P,Pt}$ = 3020 Hz) ppm. ^{77}Se NMR (52 MHz, $CDCl_3$, 25 °C, PhSeSePh): δ = 167.3 (pt) ppm.[33] MS(ESI+): *m*/*z* (%) = 874.00 (100) $[M – SePh]^+$.

[Pt(PPh$_2$Me)$_2$L1] (3): Compound **3** was prepared following a similar procedure as that described for **1** but with super hydride (1.1 mL, 1.1 mmol), **L1** (0.12 g, 0.56 mmol) and *cis*-[$PtCl_2(PPh_2Me)_2$] (0.375 g, 0.564 mmol). The resulting microcrystalline solid was collected by filtration and washed with diethyl ether to yield the product as a bright orange powder (0.3 g, 65%); m.p. 275–278 °C. $C_{38}H_{34}P_2PtS_2$ (811.84): calcd. C 56.2, H 4.2; found C 55.9, H 3.8. ^{1}H NMR (400 MHz, $CDCl_3$, 25 °C, Me_4Si): δ = 7.46 (d, $^2J_{H,H}$ = 7.3 Hz, 2 H, acenaph. 4,7-H), 7.42–7.32 (m, 8 H, P*Ph* 12,16-H), 7.32–7.24 (m, 8 H, P*Ph* 13,18-H), 7.17 (d, $^2J_{H,H}$ = 7.3 Hz, 4 H, P*Ph* 14-H), 6.85 (d, $^2J_{H,H}$ = 7.2 Hz, 2 H, acenaph. 3,8-H), 3.06 (s, 4 H, acenaph. CH_2), 1.84–1.70 (m, 6 H, PCH_3) ppm. ^{13}C NMR (67.9 MHz. $CDCl_3$; 25 °C; Me_4Si): δ = 141.9 (s), 132.8 (t, *J* = 5.5 Hz, Ph-2), 131.4 (s), 130.4 (s), 128.3 (t, *J* = 5.2 Hz), 120.4 (s), 119.5 (s), 30.3 (s), 15–14.4 (m, CH_3) ppm. ^{31}P NMR (109 MHz, $CDCl_3$, 25 °C, H_3PO_4): δ = 4.51 ($J_{P,Pt}$ = 2926 Hz) ppm. MS (ESI+): *m*/*z* (%) = 703.69 (100) $[M – SPh]^+$.

[Pt(PPh$_2$Me)$_2$L2] (4): Compound **4** was prepared by following a similar procedure to that described for **1** but with super hydride (1.1 mL, 1.1 mmol), **L2** (0.18 g, 0.56 mmol) and *cis*-[$PtCl_2(PPh_2Me)_2$] (0.38 g, 0.56 mmol). The resulting microcrystalline solid was collected by filtration and washed with diethyl ether to yield the product as an orange powder (0.2 g, 43%); m.p. 184–185 °C. $C_{38}H_{34}P_2PtSe_2$ (905.64): calcd. C 50.3, H 3.8; found C 50.3, H 3.7. ^{1}H NMR (400 MHz, $CDCl_3$, 25 °C, Me_4Si): δ = 7.82 (d, $^3J_{H,H}$ = 7.3 Hz, 2 H, acenaph. 4,7-H), 7.55–7.45 (m, 9 H, P*Ph* 14-H), 7.45–7.35 (m, 4 H, P*Ph* 12,16-H), 7.33–7.27 (m, 8 H, P*Ph* 13,18-H), 6.92 (d, $^3J_{H,H}$ = 7.2 Hz, 2 H, acenaph. 3,8-H), 3.18 (s, 4 H, acenaph. CH_2), 1.91 (s, 6 H, PCH_3) ppm. ^{13}C NMR (67.9 MHz, $CDCl_3$, 25 °C; Me_4Si): δ = 143.4 (s), 133.00–132.6 (m), 130.4 (s), 128.2 (t, *J* = 5.1 Hz), 119.3 (s), 30.1 (s), 14.9–14.7 (m, CH_3) ppm. ^{31}P NMR (162 MHz, $CDCl_3$, 25 °C, H_3PO_4): δ = 1.22 (J_{PPt} = 2958 Hz) ppm. MS(ESI+) *m*/*z* (%) = 929.07 (35) $[M + Na]^+$.

[Pt(PPhMe$_2$)$_2$L1] (5): Compound **5** was prepared by following a similar procedure to that described for **1** but with super hydride (1.1 mL, 1.1 mmol), **L1** (0.12 g, 0.56 mmol) and *cis*-[$PtCl_2(PPhMe_2)$] (0.31 g, 0.56 mmol). The resulting microcrystalline solid was collected by filtration and washed with diethyl ether to yield the product as a yellow solid (0.2 g, 50%); m.p. 265–270 °C. $C_{28}H_{30}P_2PtS_2$ (687.70): calcd. C 48.9, H 4.4; found C 48.8, H 4.3. IR (KBr disk): $\tilde{\nu}_{max}$ = 3442 (s), 3002 (w), 2908 (w), 2830 (w), 1627 (w), 1550 (w), 1479 (w), 1429 (s), 1402 (s), 1323 (w), 1293 (w), 1228 (w), 1178 (w), 1104 (w), 1033 (w), 947 (s), 906 (vs), 835 (w), 737 (w), 714 (w), 690 (w), 619 (w), 524 (w), 495 (w), 436 (w) cm^{-1}. ^{1}H NMR (400 MHz, $CDCl_3$, 25 °C, Me_4Si): δ = 7.78 (d, $^3J_{H,H}$ = 7.3 Hz, 2 H, acenaph. 4,7-H), 7.49–7.25 (m, 8 H, P*Ph* 12,16-H), 7.28 (d, ^2J = 4.4 Hz, 2 H, P*Ph* 13,18-H), 6.99 (d, $^3J_{H,H}$ = 7.2 Hz, 2 H, acenaph. 3,8-H), 3.19 (s, 4 H, acenaph. CH_2), 1.80–1.65 (m, 6 H, PCH_3) ppm. ^{13}C NMR (67.9 MHz, $CDCl_3$, 25 °C, Me_4Si): δ = 141.7 (s), 140.7 (s), 132.4 (s), 132.2 (s), 130.9 (t, *J* = 5.2 Hz), 130.3 (s), 128.5 (t, *J* = 5.1 Hz), 127.7 (t, *J* = 6.7 Hz), 119.4 (s), 30.5 (s), 13.9–13.0 (m, CH_3) ppm. ^{31}P NMR (109 MHz, $CDCl_3$, 25 °C, H_3PO_4): δ = –13.14 ($J_{P,Pt}$ = 2861, $J_{P,P}$ 8.4 Hz) ppm. MS(ESI+): *m*/*z* (%) = 578.70 $[M – SPh]^+$.

[Pt(PPhMe$_2$)$_2$L2] (6): Compound **6** was prepared by following a similar procedure to that described for **1** but with super hydride (1.1 mL, 1.1 mmol), **L2** (0.18 g, 0.56 mmol) and *cis*-[$PtCl_2(PPhMe_2)$] (0.31 g, 0.56 mmol). The resulting microcrystalline solid was collected by filtration and washed with diethyl ether to yield a yellow solid (0.2 g, 45%); m.p. 184–185 °C. $C_{28}H_{30}P_2PtSe_2$ (781.50): calcd. C 43.0, H 3.9; found C 42.8, H 3.2. ^{1}H NMR (400 MHz, $CDCl_3$, 25 °C, Me_4Si): δ = 7.88 (d, $^3J_{H,H}$ = 7.2 Hz, 2 H, acenaph. 4,7-H), 7.45–7.35 (m, 4 H, P*Ph* 12,16-H), 7.30–7.26 (m, 4 H, P*Ph* 13,18-H), 7.20 (m, 2 H, 4-H), 6.85 (d, $^3J_{H,H}$ = 7.3 Hz, 2 H, acenaph. 3,8-H), 3.09 (s, 4 H, CH_2), 1.80–1.60 (m, 12 H, PCH_3) ppm. ^{13}C NMR (67.9 MHz, $CDCl_3$, 25 °C, Me_4Si): δ = 141.7 (s), 140.7 (s), 132.4 (s), 132.2 (s), 130.8 (t, *J* = 5.2 Hz), 130.3 (s), 128.5 (t, *J* = 5.1 Hz) 127.6 (t, *J* = 6.7 Hz), 119.4 (s), 30.5 (s), 13.8–13.7 (m, CH_3) ppm. ^{31}P NMR (109 MHz, $CDCl_3$, 25 °C, H_3PO_4): δ = –16.22 ($J_{P,Pt}$ = 2895, $J_{P_A,Se}$ 67, $J_{P_A',Se}$ 40, $J_{P,P}$ 12.4 Hz) ppm. ^{77}Se NMR (52 MHz, $CDCl_3$, 25 °C, PhSeSePh): δ = 426.2 (pt) ppm.[33] MS(ESI+): *m*/*z* (%) = 625.99 (100) $[M – SePh]^+$.

Crystal Structure Analyses: X-ray crystal structures for **L1**, **L2**, and **6** were determined at –148(1) °C with the St Andrews Robotic Diffractometer,[34] a Rigaku ACTOR-SM, Saturn 724 CCD area detector with graphite monochromated Mo-K_α radiation (λ = 0.71073 Å). The data was corrected for Lorentz, polarisation and absorption effects. Data for compounds **1** and **2** were collected at –180(1) °C by using a Rigaku MM007 High brilliance RA generator (Mo-K_α radiation, confocal optic) and Saturn CCD system. At least a full hemisphere of data was collected using ω scans. Intensities were corrected for Lorentz, polarisation and absorption. Data for **5** were collected at –148(1) °C with a Rigaku SCXmini CCD area detector with graphite monochromated Mo-K_α radiation (λ = 0.71073 Å). The data were corrected for Lorentz, polarisation and absorption effects. The data for the complexes analysed was collected and processed using CrystalClear (Rigaku).[35] The structures were solved by direct methods[36] and expanded using Fourier techniques.[37] The non-hydrogen atoms were refined anisotropically. Hydrogen atoms were refined by using the riding model. All calculations were performed with the CrystalStructure[38] crystallographic software package except for refinement, which was performed with SHELXL-97.[39]

CCDC-897164 (**1**), -897165 (**2**), -897166 (**5**), -897167 (**6**), -897425 (**L1**), -897426 (**L2**) contain the supplementary crystallographic data for this paper. These data can be obtained free of charge from The Cambridge Crystallographic Data Centre via www.ccdc.cam.ac.uk/data_request/cif.

Supporting Information (see footnote on the first page of this article): Additional crystallographic information.

Acknowledgments

Mass Spectrometry was performed at the University of St. Andrews Mass Spectrometry Service by Caroline Horsburgh. The work in this project was supported by the Engineering and Physical Sciences Research Council (EPSRC).

[1] P. Kilian, F. R. Knight, J. D. Woollins, *Coord. Chem. Rev.* **2011**, *255*, 1387.
[2] C. A. Coulson, R. Daudel, J. M. Robertson, *Proc. R. Soc. London Ser. A* **1951**, *207*, 306; D. W. Cruickshank, *Acta Crystallogr.* **1957**, *10*, 504; C. P. Brock, J. D. Dunitz, *Acta Crystallogr., Sect. B: Struct. Crystallogr. Cryst. Chem.* **1982**, *38*, 2218; J. Oddershede, S. Larsen, *J. Phys. Chem. A* **2004**, *108*, 1057.
[3] A. C. Hazell, R. G. Hazell, L. Norskov-Lauritsen, C. E. Briant, D. W. Jones, *Acta Crystallogr., Sect. C: Cryst. Struct. Commun.* **1986**, *42*, 690.
[4] V. Balasubramaniyan, *Chem. Rev.* **1966**, *66*, 567.
[5] P. Kilian, F. R. Knight, J. D. Woollins, *Chem. Eur. J.* **2011**, *17*, 2302.
[6] J. D. Hoefelmeyer, M. Schulte, M. Tschinkl, F. P. Gabbai, *Coord. Chem. Rev.* **2002**, *235*, 93; L. Sobczyk, *J. Mol. Struct.* **2010**, *972*, 59; A. L. Llamas-Saiz, C. Foces-Foces, J. Elguero, *J. Mol. Struct.* **1994**, *328*, 297; H. A. Staab, T. Saupe, *Angew. Chem.* **1988**, *100*, 895; *Angew. Chem. Int. Ed. Engl.* **1988**, *27*, 865.
[7] J. Meinwald, D. Dauplaise, F. Wudl, J. J. Hauser, *J. Am. Chem. Soc.* **1977**, *99*, 255; A. J. Ashe III, J. W. Kampf, P. M. Savla, *Heteroatom Chem.* **1994**, *5*, 113; M. Lanfrey, *C. R. Acad. Sci.* **1911**, *152*, 92; W. B. Price, S. Smiles, *J. Chem. Soc.* **1928**, 2372; A. Zweig, A. K. Hoffman, *J. Org. Chem.* **1965**, *30*, 3997; P. Kilian, A. M. Z. Slawin, J. D. Woollins, *Dalton Trans.* **2006**, 2175; P. Kilian, D. Philp, A. M. Z. Slawin, J. D. Woollins, *Eur. J. Inorg. Chem.* **2003**, 249; P. Wawrzyniak, A. L. Fuller, A. M. Z. Slawin, P. Kilian, *Inorg. Chem.* **2009**, *48*, 2500.
[8] B. K. Teo, F. Wudl, J. H. Marshall, A. Krugger, *J. Am. Chem. Soc.* **1977**, *99*, 2349; B. K. Teo, P. A. Snyder-Robinson, *Inorg. Chem.* **1978**, *17*, 3489; B. K. Teo, P. A. Snyder-Robinson, *J. Chem. Soc., Chem. Commun.* **1979**, 255; B. K. Teo, P. A. Snyder-Robinson, *Inorg. Chem.* **1979**, *18*, 1490; B. K. Teo, P. A. Snyder-Robinson, *Inorg. Chem.* **1981**, *20*, 4235; B. K. Teo, P. A. Snyder-Robinson, *Inorg. Chem.* **1984**, *23*, 32.
[9] B. K. Teo, F. Wudl, J. J. Hauser, A. Krugger, *J. Am. Chem. Soc.* **1977**, *99*, 4862; B. K. Teo, V. Bakirtzis, P. A. Snyder-Robinson, *J. Am. Chem. Soc.* **1983**, *105*, 6330.
[10] W. P. Bosman, H. G. M. van der Linden, *J. Chem. Soc., Chem. Commun.* **1977**, 714.
[11] A. W. Gal, J. W. Gosselink, F. A. Vollenbroek, *Inorg. Chim. Acta* **1979**, *32*, 235.
[12] S. M. Aucott, H. L. Milton, S. D. Robertson, A. M. Z. Slawin, G. D. Walker, J. D. Woollins, *Chem. Eur. J.* **2004**, *10*, 1666.
[13] S. M. Aucott, H. L. Milton, S. D. Robertson, A. M. Z. Slawin, J. D. Woollins, *Dalton Trans.* **2004**, 3347.
[14] S. M. Aucott, D. Duerden, Y. Li, A. M. Z. Slawin, J. D. Woollins, *Chem. Eur. J.* **2006**, *12*, 5495.
[15] S. D. Robertson, A. M. Z. Slawin, J. D. Woollins, *Eur. J. Inorg. Chem.* **2007**, 247.
[16] H. Xu, J. H. K. Yip, *Inorg. Chem.* **2003**, *42*, 4492.
[17] M. Tesmer, H. Vahrenkamp, *Eur. J. Inorg. Chem.* **2001**, 1183.
[18] S. M. Aucott, P. Kilian, H. L. Milton, S. D. Robertson, A. M. Z. Slawin, J. D. Woollins, *Inorg. Chem.* **2005**, *44*, 2710.
[19] S. D. Robertson, A. M. Z. Slawin, J. D. Woollins, *Polyhedron* **2006**, *25*, 823.
[20] M.-L. Lechner, K. S. Athukorala Arachchige, R. A. M. Randall, F. R. Knight, M. Bühl, A. M. Z. Slawin, J. D. Woollins, *Organometallics* **2012**, *31*, 2922.
[21] L. K. Aschenbach, F. R. Knight, R. A. M. Randall, D. B. Cordes, A. Baggott, M. Bühl, A. M. Z. Slawin, J. D. Woollins, *Dalton Trans.* **2012**, *41*, 3141.
[22] F. R. Knight, R. A. M. Randall, L. Wakefield, A. M. Z. Slawin, J. D. Woollins, *Inorg. Chem.* **2012**, *51*, 11087; F. R. Knight, R. A. M. Randall, L. Wakefield, A. M. Z. Slawin, J. D. Woollins, *Dalton Trans.* **2012**, DOI: 001:10.1039/C2DT31390A.
[23] Y. Aso, K. Yui, T. Miyoshi, T. Otsubo, F. Ogura, J. Tanaka, *Bull. Chem. Soc. Jpn.* **1988**, *61*, 2013.
[24] W. D. Neudorff, D. Lentz, M. Anibarro, A. D. Schlüter, *Chem. Eur. J.* **2003**, *9*, 2745.
[25] J. A. Iggo (Ed.), *NMR Spectroscopy in Inorganic Chemistry*, Oxford University Press Inc., New York, **1999**.
[26] W. H. Hersh, *J. Chem. Educ.* **1997**, *74*, 1485.
[27] C. P. Morley, C. A. Webster, P. Douglas, K. Rofe, M. Di Vaira, *Dalton Trans.* **2010**, *39*, 3177.
[28] A. Bondi, *J. Phys. Chem.* **1964**, *68*, 441.
[29] S. M. Aucott, H. L. Milton, S. D. Robertson, A. M. Z. Slawin, J. D. Woollins, *Heteroat. Chem.* **2004**, *15*, 530.
[30] C. A. Tolman, *Chem. Rev.* **1977**, *77*, 313.
[31] H. W. Roesky, M. Andruh, *Coord. Chem. Rev.* **2003**, *236*, 91; T. Koizumi, K. Tsutsui, K. Tanaka, *Eur. J. Org. Chem.* **2003**, 4528; C. Janiak, *J. Chem. Soc., Dalton Trans.* **2000**, 3885.
[32] M. Nishio, *CrystEngComm* **2004**, *6*, 130; C. Fischer, T. Gruber, W. Seichter, D. Schindler, E. Weber, *Acta Crystallogr., Sect. E* **2008**, *64*, o673; M. Hirota, K. Sakaibara, H. Suezawa, T. Yuzuri, E. Ankai, M. Nishio, *J. Phys. Org. Chem.* **2000**, *13*, 620; H. Tsubaki, S. Tohyama, K. Koike, H. Saitoh, O. Ishitani, *Dalton Trans.* **2005**, 385.
[33] pt stands for pseudotriplet and represents the coupling of a ^{77}Se nucleus to the *cis* and *trans* ^{31}P nuclei, in which the central peaks overlap. As such calculation of the coupling constants was not possible.
[34] A. L. Fuller, L. A. S. Scott-Hayward, Y. Li, M. Bühl, A. M. Z. Slawin, J. D. Woollins, *J. Am. Chem. Soc.* **2010**, *132*, 5799.
[35] a) *CrystalClear*, v. 1.6, Rigaku Corporation, **1999**; b) J. W. P. Flugrath, *Acta Crystallogr., Sect. D* **1999**, *55*, 1718.

[36] SIR97: A. Altomare, M. Burla, M. Camalli, G. Cascarano, C. Giacovazzo, A. Guagliardi, A. Moliterni, G. Polidori, R. Spagna, *J. Appl. Crystallogr.* **1999**, *32*, 115.
[37] P. T. Beurskens, G. Admiraal, G. Beurskens, W. P. Bosman, R. de Gelder, R. Israel, J. M. M. Smits, *DIRDIF99*, *Technical Report of the Crystallography Laboratory*, University of Nijmegen, The Netherlands, **1999**.
[38] *CrystalStructure*, v. 3.8.1, *Crystal Structure Analysis Package*, Rigaku and Rigaku/MSC, Texas, USA, **2000**–**2006**.
[39] *SHELX97*, see: G. M. Sheldrick, *Acta Crystallogr., Sect. A* **2008**, *64*, 112.

Received: August 22, 2012
Published Online: November 26, 2012

